Inorg. Chem. **1982**, *21*, 2667-2675 **2667**

Contribution from the Department of Chemistry,
Texas A&M University, College Station, Texas 77843

Structures of Two Dirhodium(II) Compounds Containing Hydrogen-Bonded Nitroxyl Groups: Tetrakis(trifluoroacetato)bis(2,2,6,6-tetramethyl-4-hydroxypiperidinyl-1-oxy)dirhodium(II) and Tetrakis(trifluoroacetato)diaquadirhodium(II) Di-*tert*-butyl Nitroxide Solvate

F. ALBERT COTTON* and TIMOTHY R. FELTHOUSE

Received November 19, 1981

The crystal and molecular structures have been determined by single-crystal X-ray diffraction techniques for the following two compounds: $Rh_2(O_2CCF_3)_4(Tempol)_2$ (**1**) and $Rh_2(O_2CCF_3)_4(H_2O)_2\cdot 2DTBN$ (**2**) (Tempol = 2,2,6,6-tetramethyl-4-hydroxypiperidinyl-1-oxy and DTBN = di-*tert*-butyl nitroxide). Compound **1** crystallizes as dark blue prisms in the space group $P2_1/n$ with two dinuclear molecules residing on crystallographic centers of inversion in a cell of dimensions a = 8.4087 (6) Å, b = 19.5393 (19) Å, c = 12.1912 (10) Å, β = 107.785 (7)°, and V = 1907.3 (7) Å^3. The structure was solved by the heavy-atom Patterson method and refined with use of 3112 data with $I > 3\sigma(I)$ to final discrepancy indices of R_1 = 0.035 and R_2 = 0.046 with the inclusion of all hydrogen atoms. Four trifluoroacetate groups span the Rh–Rh bond of length 2.405 (1) Å; the axial positions are occupied by Tempol ligands, each coordinated at 2.240 (3) Å through the 4-hydroxyl oxygen atom, O(5). The Rh′–Rh–O(5) angle is slightly distorted from linearity with a value of 176.39 (8)°. The piperidine rings of the Tempol ligands in **1** adopt a chair conformation with the N–O bond making an angle of 18.6° with the C_2N plane. The nitroxyl oxygen atoms participate in intermolecular hydrogen bonding with the hydroxyl groups from adjacent dinuclear molecules linking the $Rh_2(O_2CCF_3)_4(Tempol)_2$ molecules into zigzag chains through the crystal. Compound **2** crystallizes as dichroic irregularly shaped prisms in the space group $P\bar{1}$ with one formula unit located on a crystallographic center of inversion in a unit cell of dimensions a = 10.3765 (20) Å, b = 12.1955 (10) Å, c = 8.4080 (9) Å, α = 101.442 (8)°, β = 109.167 (14)°, γ = 99.439 (11)°, and V = 954.4 (6) Å^3. The structure was solved by conventional Patterson, Fourier, and least-squares refinement techniques using 3181 data with $I > 3\sigma(I)$ to R_1 and R_2 values of 0.032 and 0.046, respectively. All hydrogen atoms were included in the refinement. The structure is comprised of $Rh_2(O_2CCF_3)_4(H_2O)_2$ and DTBN molecules with the four trifluoroacetate groups bridging in conventional fashion the Rh–Rh bond of length 2.409 (1) Å. Water molecules occupy the axial positions at 2.243 (2) Å from the Rh atoms. The water hydrogen atoms participate in hydrogen-bonding interactions with the nitroxyl oxygen atoms of the DTBN molecules. Two DTBN molecules are found for each dirhodium unit, and these are situated between neighboring $Rh_2(O_2CCF_3)_4(H_2O)_2$ molecules. Only one genuine hydrogen bond is formed for each hydrogen atom of the water molecule, although a number of other close contacts exist. The C_2NO group of the nitroxide molecule is nearly planar with the N–O bond making an angle of only 0.7° with the C_2N plane. A detailed examination of the structural parameters in eight $Rh_2(O_2CCF_3)_4L_2$ complexes reveals that the trifluoroacetate bridging groups are essentially unchanged in dimensions upon substitution of a variety of axial donor ligands with the only significant structural changes occurring as a consequence of variations in the L–Rh–Rh–L bonding. The intermolecular hydrogen bonding in **1** and **2** closely resembles that observed in structures of organic nitroxide compounds.

Introduction

During the past decade, a vast number of studies have been undertaken on tetrakis(carboxylato) complexes of the transition elements containing metal-to-metal bonds.[1,2] Naturally, a change in the metal atoms or their valence state alters the chemical and electronic properties of $M_2(O_2CR)_4L_2$ type compounds. These properties may also be very effectively altered by changes in the identity of the R group or the axial donor ligand, L. Substitution of R = CF_3 for CH_3 in the group 6B tetracarboxylates causes pronounced variations in the chemical and structural characteristics of these compounds. The Cr–Cr distance of 2.541 (1) Å in $Cr_2(O_2CCF_3)_4(Et_2O)_2$[3] represents an upper limit[4] among known quadruply bonded dichromium(II) compounds, while in $Cr_2(O_2CCH_3)_4(H_2O)_2$[5] the Cr–Cr bond length is nearly 0.2 Å shorter with a value of 2.362 (1) Å. In $Mo_2(O_2CR)_4$ complexes the Mo–Mo bond length varies less as a function of R, but in contrast to the acetate analogue, $Mo_2(O_2CCF_3)_4$[6] exhibits greater solubility in organic solvents, higher volatility,[7] enhanced affinity for axial donor ligands,[8] and, with certain tertiary phosphine ligands, the ability to form equatorial phosphine complexes containing both bidentate and monodentate trifluoroacetate groups.[9,10] The marked thermal stability displayed by $Mo_2(O_2CCF_3)_4$ was recently found to extend to the W_2^{4+} analogue in the form of $W_2(O_2CCF_3)_4\cdot{}^2/_3$(diglyme).[11] This compound is sufficiently stable to allow both purification and crystallization by means of sublimation. Furthermore, the compound provides the first example of a tetrakis(carboxylato) complex of ditungsten(II) despite more than 20 years of efforts.[12]

Although the first trifluoroacetate complex of Rh_2^{4+} was reported in 1963,[13] structural data on $Rh_2(O_2CCF_3)_4L_2$ com-

---

(1) (a) For recent reviews see: Cotton, F. A.; Walton, R. A. "Multiple Bonds Between Metal Atoms"; Wiley: New York, 1982. (b) Porai-Koshits, M. A. *Zh. Strukt. Khim.* **1980**, *21*, 146; *J. Struct. Chem.* (*Engl. Transl.*) **1980**, *21*, 369. (c) Templeton, J. L. *Prog. Inorg. Chem.* **1979**, *26*, 211. (d) Cotton, F. A. *Acc. Chem. Res.* **1978**, *11*, 225. (e) Baranovskii, I. B.; Shchelokov, R. N. *Zh. Neorg. Khim.* **1978**, *23*, 3; *Russ. J. Inorg. Chem.* (*Engl. Transl.*) **1978**, *23*, 1.

(2) For reviews on specific elements see: (a) Bino, A.; Cotton, F. A. *Chem. Uses Molybdenum, Proc. Int. Conf., 3rd* **1979**, 1 (molybdenum). (b) Dori, Z. *Prog. Inorg. Chem.* **1981**, *28*, 239 (tungsten). (c) Felthouse, T. R. *Prog. Inorg. Chem.* **1982**, *29*, 73 (rhodium).

(3) Cotton, F. A.; Extine, M. W.; Rice, G. W. *Inorg. Chem.* **1978**, *17*, 176.

(4) Cotton, F. A.; Ilsley, W. H.; Kaim, W. *J. Am. Chem. Soc.* **1980**, *102*, 3464.

(5) Cotton, F. A.; DeBoer, B. G.; LaPrade, M. D.; Pipal, J. R.; Ucko, D. A. *Acta Crystallogr., Sect. B* **1971**, *B27*, 1664.

(6) Cotton, F. A.; Norman, J. G., Jr. *J. Coord. Chem.* **1971**, *1*, 161.

(7) A consequence of this high volatility has been the determination of the gas-phase structure by electron diffraction: Garner, C. D.; Hillier, I. H.; Walton, I. B.; Beagley, B. *J. Chem. Soc., Dalton Trans.* **1979**, 1279.

(8) Cotton, F. A.; Norman, J. G., Jr. *J. Am. Chem. Soc.* **1972**, *94*, 5697.

(9) Girolami, G. S.; Mainz, V. V.; Andersen, R. A. *Inorg. Chem.* **1980**, *19*, 805.

(10) Cotton, F. A.; Lay, D. G. *Inorg. Chem.* **1981**, *20*, 935.

(11) Sattelberger, A. P.; McLaughlin, K. W.; Huffman, J. C. *J. Am. Chem. Soc.* **1981**, *103*, 2880.

(12) Abel, E. W.; Singh, A.; Wilkinson, G. *J. Chem. Soc.* **1959**, 3097.

0020-1669/82/1321-2667$01.25/0

plexes were not available until very recently.[14] However, work by Kitchens and Bear[15,16] in 1970 established that $Rh_2(O_2CCF_3)_4$, like its group 6B analogues, showed a tendency to remain intact in the gas phase as evidenced by the observation[15] of a parent ion for $Rh_2(O_2CCF_3)_4$ in the mass spectrum. The corresponding acetate,[16] propionate,[15] and benzoate[15] complexes of Rh_2^{4+} decompose at elevated temperatures to give metallic rhodium (R = CH_3, C_2H_5) or oxide compounds (R = Ph). Further studies of $Rh_2(O_2CCF_3)_4$ have revealed that electrochemical oxidation to the $Rh_2(O_2CCF_3)_4^+$ cation radical does not occur in CH_2Cl_2 solutions[17] although these radicals can be generated for the phosphorus-donor adducts in Freon glasses by γ irradiation.[18] This behavior toward oxidation is in accord with the general ability of the trifluoroacetate group to stabilize the lower oxidation states of elements of the transition series as well as those of the main groups.[19]

In addition to the effect on the thermal and redox properties of $Rh_2(O_2CCF_3)_4$ compared to those of other alkyl or aryl carboxylate complexes of Rh_2^{4+}, the trifluoroacetate group also exerts a strong influence on the type and strength of interaction with axial donor atoms in $Rh_2(O_2CCF_3)_4L_2$ compounds. Dimethyl sulfoxide (Me_2SO) coordinates to the Rh atoms in $Rh_2(O_2CR)_4(Me_2SO)_2$ complexes (R = CH_3,[20] C_2H_5[21]) through the sulfur atoms, but in the case of $Rh_2(O_2CCF_3)_4(Me_2SO)_2$,[21,22] axial ligation occurs through the oxygen atoms. The highly electronegative CF_3 substituents enhance the Lewis acidity of the Rh atoms so as to allow axial interactions with relatively weak donor molecules. Dimethyl sulfone (Me_2SO_2) normally does not coordinate to transition-metal ions[23] but forms a 2:1 adduct with $Rh_2(O_2CCF_3)_4$.[24]

Table I. Summary of Crystallographic Data and Data Collection Procedures for the Two Compounds

parameter	1	2
formula	$Rh_2F_{12}O_{12}N_2C_{26}H_{36}$	$Rh_2F_{12}O_{12}N_2C_{24}H_{40}$
space group	$P2_1/n$	$P\bar{1}$
a, Å	8.4087 (6)	10.3765 (20)
b, Å	19.5393 (19)	12.1955 (10)
c, Å	12.1912 (10)	8.4080 (9)
α, deg	90.0	101.442 (8)
β, deg	107.785 (7)	109.167 (14)
γ, deg	90.0	99.439 (11)
V, Å^3	1907.3 (7)	954.4 (6)
d_{calcd}, g cm^{-3}	1.74	1.71
Z	2	1
fw	1002.37	982.38
cryst size, mm	0.25 × 0.27 × 0.52	0.10 × 0.15 × 0.30
μ(Mo Kα), cm^{-1}	9.659	9.628
radiation	graphite-monochromated Mo K$\bar{\alpha}$ ($\lambda_{\bar{\alpha}}$ = 0.710 73 Å)	
scan type	ω–2θ	ω–2θ
scan width ($\Delta\omega$), deg	0.70 + 0.35 tan θ	0.60 + 0.35 tan θ
aperture width, mm	1.5 + tan θ	1.5 + tan θ
max scan speed, deg min^{-1}	20.12	20.12
max counting time, s	30	30
data collection range	$+h, +k, \pm l$; $3° \leqslant 2\theta \leqslant 55°$	$+h, \pm k, \pm l$; $4° \leqslant 2\theta \leqslant 52°$
no. of unique data	4354	3726
no. of data, $F_o^2 > 3\sigma(F_o^2)$	3112	3181
p	0.05	0.05
X-ray exposure time, h	35.5	30.1
no. of intensity stds	3	3
time between measmts, s	3600	3600
cryst dec	negligible	negligible
no. of variables	316	295
R_1	0.035	0.032
R_2	0.046	0.046
esd	1.318	1.439
largest peak,[a] e Å^{-3}	0.42	0.46
$\Delta:\sigma$[b]	0.07	0.53

[a] Largest peak in the final difference Fourier map. [b] Largest shift (Δ) to error (σ) ratio in the final least-squares cycle.

Nitroxyl radicals constitute another class of donor ligands that have been used to assess directly the metal–ligand bonding via EPR spectroscopy.[25] Although in most cases the nitroxyl radical is not directly coordinated to the metal ion, sufficiently strong Lewis acid sites form complexes with the oxygen atom of the nitroxide group.[26-29] Structural data are available for the 2,2,6,6-tetramethyl-4-hydroxypiperidinyl-1-oxy[28] (Tempol) and 2,2,6,6-tetramethylpiperidinyl-1-oxy[29] (Tempo) complexes with $Cu(hfac)_2$. Several years ago, Drago et al.[27] reported that $Rh_2(O_2CCF_3)_4$, and not the corresponding butyrate complex, forms a 1:1 adduct in solution with 2,2,6,6-tetramethylpiperidinyl-1-oxy (Tempo). Somewhat surprisingly, hyperfine coupling to only one of the rhodium atoms was observed, suggesting a rather limited amount of spin delocalization onto the Rh_2^{4+} moiety. As an alternative means of assessing the degree of spin delocalization across the dirhodium(II) unit, we sought to prepare a 2:1 adduct of $Rh_2(O_2CCF_3)_4$ with suitable nitroxide ligands. These adducts, however, do not rule out some degrees of superexchange through the bridging trifluoroacetate groups. We began our study by investigating the structures of $Rh_2(O_2CCF_3)_4$ adducts of di-*tert*-butyl nitroxide (DTBN) and Tempol. With both nitroxides crystalline products were obtained containing the nitroxide ligand and the $Rh_2(O_2CCF_3)_4$ unit in a 2:1 ratio. In each compound the nitroxide avoids direct coordination to the Rh atoms and instead participates in hydrogen-bonding interactions throughout the crystal lattice.

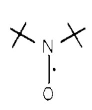

DTBN

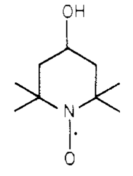

Tempol

Experimental Section

Compound Preparation. Rhodium(II) trifluoroacetate was prepared by a method given by Kitchens and Bear[15] and was converted to the anhydrous form before use by heating at 150 °C for 30 min.

$Rh_2(O_2CCF_3)_4(Tempol)_2$ (**1**) was prepared by mixing benzene solutions of $Rh_2(O_2CCF_3)_4$ (0.05 g, 7.6 × 10^{-5} mol) and Tempol (Sigma, 0.05 g, 2.9 × 10^{-4} mol, a 2-fold excess) to give a blue-green powder, which was collected by filtration and washed with benzene.

---

[13] Johnson, S. A.; Hunt, H. R.; Neumann, H. M. *Inorg. Chem.* **1963**, *2*, 960.
[14] Porai-Koshits, M. A.; Dikareva, L. M.; Sadikov, G. G.; Baranovskii, I. B. *Zh. Neorg. Khim.* **1979**, *24*, 1286; *Russ. J. Inorg. Chem.* (*Engl. Transl.*) **1979**, *24*, 716.
[15] Kitchens, J.; Bear, J. L. *Thermochim. Acta* **1970**, *1*, 537.
[16] Kitchens, J.; Bear, J. L. *J. Inorg. Nucl. Chem.* **1970**, *32*, 49.
[17] Das, K.; Kadish, K. M.; Bear, J. L. *Inorg. Chem.* **1978**, *17*, 930.
[18] Kawamura, T.; Fukamachi, K.; Sowa, T.; Hayashida, S.; Yonezawa, T. *J. Am. Chem. Soc.* **1981**, *103*, 364.
[19] Garner, C. D.; Hughes, B. *Adv. Inorg. Chem. Radiochem.* **1975**, *17*, 1.
[20] Cotton, F. A.; Felthouse, T. R. *Inorg. Chem.* **1980**, *19*, 323.
[21] Cotton, F. A.; Felthouse, T. R. *Inorg. Chem.* **1980**, *19*, 2347.
[22] Cotton, F. A.; Felthouse, T. R. *Inorg. Chem.* **1982**, *21*, 431.
[23] The strategy of using CF_3 groups to enhance the Lewis acidity of the metal center has been used in several mononuclear complexes of hexafluoroacetylacetonate (hfac). A variety of oxygen bases in chloroform form adducts with $UO_2(hfac)_2$, including sulfones, but no solid adducts with these sulfone ligands were reported: Kramer, G. M.; Maas, E. T., Jr.; Dines, M. B. *Inorg. Chem.* **1981**, *20*, 1415.
[24] Cotton, F. A.; Felthouse, T. R. *Inorg. Chem.* **1981**, *20*, 2703.
[25] Eaton, S. S.; Eaton, G. R. *Coord. Chem. Rev.* **1978**, *26*, 207.
[26] Hoffman, B. M.; Eames, T. B. *J. Am. Chem. Soc.* **1969**, *91*, 5168.
[27] Richman, R. M.; Kuechler, T. C.; Tanner, S. P.; Drago, R. S. *J. Am. Chem. Soc.* **1977**, *99*, 1055.
[28] Anderson, O. P.; Kuechler, T. C. *Inorg. Chem.* **1980**, *19*, 1417.
[29] Dickman, M. H.; Doedens, R. J. *Inorg. Chem.* **1981**, *20*, 2677.

Table II. Atomic Positional Parameters for $Rh_2(O_2CCF_3)_4(Tempol)_2$ (1)[a]

atom	x	y	z
Rh	0.05518 (3)	0.05524 (1)	0.03561 (2)
F(1)	0.0784 (6)	0.1058 (2)	−0.3315 (3)
F(2)	−0.1387 (6)	0.0554 (3)	−0.3864 (3)
F(3)	0.0677 (7)	0.0074 (3)	−0.3725 (3)
F(4)	−0.5103 (4)	0.1174 (2)	−0.0356 (3)
F(5)	−0.5880 (4)	0.0340 (2)	−0.1414 (4)
F(6)	−0.4816 (4)	0.1183 (2)	−0.2001 (3)
O(1)	−0.0365 (3)	−0.0276 (1)	−0.1920 (2)
O(2)	0.0650 (3)	0.0768 (1)	−0.1258 (2)
O(3)	−0.2859 (3)	−0.0123 (1)	−0.0835 (2)
O(4)	−0.1828 (3)	0.0917 (1)	−0.0147 (2)
O(5)	0.1718 (4)	0.1548 (2)	0.1096 (2)
O(6)	0.6314 (5)	0.2163 (2)	0.5255 (2)
N	0.5238 (4)	0.2031 (2)	0.4278 (3)
C(1)	0.0132 (4)	0.0316 (2)	−0.2008 (3)
C(2)	0.0073 (6)	0.0519 (3)	−0.3232 (3)
C(3)	−0.2953 (5)	0.0502 (2)	−0.0646 (3)
C(4)	−0.4705 (6)	0.0827 (3)	−0.1114 (4)
C(5)	0.2987 (5)	0.1556 (2)	0.2192 (3)
C(6)	0.4466 (6)	0.1986 (2)	0.2168 (3)
C(7)	0.5901 (5)	0.1944 (2)	0.3290 (4)
C(8)	0.7116 (7)	0.2537 (3)	0.3352 (5)
C(9)	0.6833 (7)	0.1261 (3)	0.3391 (5)
C(10)	0.3591 (6)	0.1764 (2)	0.4330 (4)
C(11)	0.3818 (8)	0.1026 (3)	0.4774 (4)
C(12)	0.3036 (8)	0.2201 (4)	0.5177 (5)
C(13)	0.2318 (6)	0.1810 (2)	0.3122 (4)

[a] Estimated standard deviations for the least significant figures are given in parentheses and are given in this fashion in succeeding tables.

The powder was then suspended in a benzene solution, and acetone was added dropwise until the powder dissolved. Slow evaporation of the solution readily gave dark blue, blocky crystals.

The DTBN complex was first prepared by the addition of $Rh_2(O_2CCF_3)_4$ (0.05 g, 7.6×10^{-5} mol) to a 20-mL solution of 1:1 benzene–chloroform containing DTBN (Eastman, 0.2 g, 1.4×10^{-3} mol, a 9-fold excess). The solution was covered with Parafilm containing several pinholes and allowed to evaporate slowly over a 1-week period. The resulting dark green crystals were extremely soluble in the solvent mixture and only formed after nearly all the solvent had evaporated. Unfortunately, all these crystals were found to be badly twinned even though numerous attempts were made to cleave a single crystal from the crystalline mass which had formed. The crystalline dark green solid was redissolved in benzene–chloroform containing a few drops of DTBN and evaporated with exposure to moist air. This time the crystals that formed upon evaporation of the solvent were irregularly shaped dichroic blue–red prisms. Subsequent analysis by X-ray diffraction (vide infra) showed these crystals to be $Rh_2(O_2CCF_3)_4(H_2O)_2 \cdot 2DTBN$ (**2**).

X-ray Crystallography. Data Collection, Structure Solution, and Refinement.[30] Suitable crystals of **1** and **2** were secured with epoxy cement on glass fibers and mounted on an Enraf-Nonius CAD-4F autodiffractometer. Crystallographic data and data collection parameters are summarized in Table I for both compounds. Details of the data collection techniques and derivation of the intensity and its standard deviation have appeared before[31] for this diffractometer. For **2** an empirical absorption correction was made using ψ scans (ψ = 0–360° every 10° for χ values near 90°). Nine sets of reflections ($\bar{6}\bar{3}2$, $\bar{6}2\bar{1}$, $\bar{5}\bar{3}2$, $\bar{4}\bar{3}1$, $\bar{4}\bar{1}0$, $\bar{3}\bar{2}1$, $\bar{8}\bar{4}3$, $\bar{8}\bar{3}1$, $\bar{6}\bar{4}2$) were averaged to give an absorption profile for the crystal with maximum, minimum, and average transmission factors of 1.00, 0.91, and 0.97, respectively.

The structures of **1** and **2** were solved straightforwardly with heavy-atom methods from three-dimensional Patterson maps, which revealed the positions of the Rh atoms, followed by successive least-squares refinement and difference Fourier maps. In both structures a difference Fourier map following least-squares refinement of the nonhydrogen atoms with anisotropic thermal parameters assigned to these atoms revealed the positions of all hydrogen atoms. The 18 hydrogen atoms in **1** were refined with isotropic thermal parameters, while in **2** only the positional parameters were refined for the 20 hydrogen atoms. An extinction correction was made in **2** according to the equation $|F_o| = |F_c|(1 + gI_c)^{-1}$, where the value of g determined by least-squares refinement is 8.61×10^{-7}. This parameter was not varied in the final cycle. Tables of observed and calculated structure factor amplitudes for those reflections with $I > 3\sigma(I)$ are available for the two structures.[32]

Table III. Atomic Positional Parameters for $Rh_2(O_2CCF_3)_4(H_2O)_2 \cdot 2DTBN$ (**2**)

atom	x	y	z
Rh	0.11699 (2)	0.48813 (2)	0.02147 (3)
F(1)	0.0271 (2)	0.6354 (2)	0.5881 (2)
F(2)	0.2337 (3)	0.6235 (3)	0.6224 (3)
F(3)	0.1630 (3)	0.7632 (2)	0.5388 (3)
F(4)	0.2133 (4)	0.8563 (2)	−0.0670 (4)
F(5)	0.0384 (4)	0.8885 (2)	−0.0348 (6)
F(6)	0.2045 (5)	0.8899 (2)	0.1702 (5)
O(1)	0.1685 (2)	0.5536 (2)	0.2826 (3)
O(2)	−0.0500 (2)	0.5777 (2)	0.2425 (3)
O(3)	0.1710 (2)	0.6535 (2)	0.0103 (3)
O(4)	−0.0481 (2)	0.6761 (2)	−0.0320 (3)
O(5)	0.3363 (2)	0.4679 (2)	0.0677 (3)
O(6)	0.5703 (3)	0.6541 (2)	0.1698 (3)
N	0.6229 (3)	0.7499 (2)	0.2843 (4)
C(1)	0.0754 (3)	0.5870 (3)	0.3298 (4)
C(2)	0.1249 (4)	0.6530 (3)	0.5228 (4)
C(3)	0.0787 (3)	0.7089 (3)	−0.0070 (4)
C(4)	0.1306 (4)	0.8373 (3)	0.0128 (5)
C(10)	0.6295 (5)	0.7458 (4)	0.4631 (5)
C(11)	0.4977 (7)	0.7739 (10)	0.4774 (8)
C(12)	0.7631 (7)	0.8231 (6)	0.6086 (7)
C(13)	0.6461 (10)	0.6246 (6)	0.4759 (9)
C(20)	0.6706 (4)	0.8497 (3)	0.2226 (5)
C(21)	0.6307 (6)	0.9570 (4)	0.2967 (9)
C(22)	0.8260 (6)	0.8707 (6)	0.2650 (9)
C(23)	0.5937 (10)	0.8206 (5)	0.0296 (8)

Results

The final values for the atomic positional parameters are presented in Tables II and III for compounds **1** and **2**, respectively. Tables IIA and IIIA[32] give anisotropic thermal parameters and refined hydrogen atom positions with isotropic thermal parameters for the two compounds. Bond distances and angles for the nonhydrogen atoms in **1** and **2** appear in Tables IV and V, respectively, and some hydrogen-bonding contacts for these atoms are included as well. Intra- and interatomic hydrogen distances and angles for **1** and **2** are compiled in Tables IVA and VA,[32] respectively. Selected least-squares planes and dihedral angles for the two compounds are tabulated in Table VI.[32] Both structures contain dinuclear $Rh_2(O_2CCF_3)_4$ molecules with symmetrically bridging trifluoroacetate groups and nitroxide radicals in a 1:2 ratio. A detailed description of each structure will now be given.

$Rh_2(O_2CCF_3)_4(Tempol)_2$ (1). Two formula units of **1** comprise the unit cell with crystallographic centers of inversion located at the midpoints of the Rh–Rh bonds. Figure 1 shows the atom-labeling scheme for one of the dinuclear molecules. Four trifluoroacetate groups symmetrically bridge the Rh–Rh bond of length 2.405 (1) Å. The central $Rh_2(O_2CC)_4$ core of **1** displays essentially D_{4h} symmetry. Each Rh atom is in a tetragonally elongated octahedral environment and is displaced 0.070 Å out of the equatorial plane of four carboxylate oxygen atoms toward the axial hydroxyl oxygen atom. Some chemically equivalent bond distances and angles within the $Rh_2(O_2CCF_3)_4$ unit include the following: Rh–O, 2.034 (3) Å; C–O, 1.250 (5) Å; C–CF_3, 1.537 (6) Å; C–F, 1.266 (6) Å; ∠Rh′–Rh–O(trifluoroacetate), 88.02 (8)°; ∠Rh–O–C(tri-

---

(30) All crystallographic computing was done on a linked PDP 11/45-11/60 computer at the Molecular Structure Corp., College Station, TX, with the Enraf-Nonius structure determination package with local modifications.

(31) Bino, A.; Cotton, F. A.; Fanwick, P. E. *Inorg. Chem.* **1979**, *18*, 3558.

(32) Supplementary material.

Table IV. Bond Distances (Å) and Angles (Deg) for $Rh_2(O_2CCF_3)_4(Tempol)_2$ (**1**) Excluding the Hydrogen Atoms[a]

Rh-Rh'	2.405 (1)	O(5)-C(5)	1.433 (4)
Rh-O(1')	2.033 (2)	O(5)···O(6'')	2.702 (4)
Rh-O(2)	2.039 (2)	O(6)-N	1.282 (4)
Rh-O(3')	2.029 (2)	N-C(7)	1.483 (5)
Rh-O(4)	2.034 (3)	N-C(10)	1.499 (6)
Rh-O(5)	2.240 (3)	C(1)-C(2)	1.530 (5)
F(1)-C(2)	1.231 (5)	C(3)-C(4)	1.544 (6)
F(2)-C(2)	1.236 (6)	C(5)-C(6)	1.508 (6)
F(3)-C(2)	1.250 (6)	C(5)-C(13)	1.497 (6)
F(4)-C(4)	1.271 (6)	C(6)-C(7)	1.525 (5)
F(5)-C(4)	1.340 (6)	C(7)-C(8)	1.531 (7)
F(6)-C(4)	1.265 (6)	C(7)-C(9)	1.533 (7)
O(1)-C(1)	1.245 (4)	C(10)-C(11)	1.532 (7)
O(2)-C(1)	1.250 (4)	C(10)-C(12)	1.518 (7)
O(3)-C(3)	1.250 (5)	C(10)-C(13)	1.536 (6)
O(4)-C(3)	1.254 (5)		

Rh'-Rh-O(1')	88.16 (7)	F(1)-C(2)-C(1)	115.4 (4)
-O(2)	87.82 (7)	F(2)-C(2)-F(3)	102.3 (5)
-O(3')	87.82 (7)	F(2)-C(2)-C(1)	110.6 (4)
-O(4)	88.29 (8)	F(3)-C(2)-C(1)	113.1 (4)
-O(5)	176.39 (8)	O(3)-C(3)-O(4)	129.9 (3)
O(1')-Rh-O(2)	175.94 (9)	O(3)-C(3)-C(4)	116.1 (4)
-O(3')	87.8 (1)	O(4)-C(3)-C(4)	114.0 (4)
-O(4)	91.4 (1)	F(4)-C(4)-F(5)	103.9 (4)
-O(5)	90.2 (1)	-F(6)	111.2 (5)
O(2)-Rh-O(3')	92.6 (1)	-C(3)	112.6 (4)
-O(4)	87.9 (1)	F(5)-C(4)-F(6)	107.5 (5)
-O(5)	93.9 (1)	-C(3)	110.5 (4)
O(3')-Rh-O(4)	176.1 (1)	F(6)-C(4)-C(3)	110.8 (4)
-O(5)	88.9 (1)	O(5)-C(5)-C(6)	111.8 (3)
O(4)-Rh-O(5)	94.9 (1)	O(5)-C(5)-C(13)	111.4 (4)
Rh'-O(1)-C(1)	116.9 (2)	C(6)-C(5)-C(13)	109.4 (3)
Rh-O(2)-C(1)	116.9 (2)	C(5)-C(6)-C(7)	112.6 (3)
Rh'-O(3)-C(3)	117.4 (2)	N-C(7)-C(6)	109.3 (3)
Rh-O(4)-C(3)	116.5 (2)	N-C(7)-C(8)	106.5 (4)
Rh-O(5)-C(5)	119.6 (2)	N-C(7)-C(9)	110.1 (4)
O(6'')···O(5)-C(5)	108.4 (2)	C(6)-C(7)-C(8)	109.7 (4)
O(5'')···O(6)-N	120.8 (2)	-C(9)	111.3 (4)
O(6)-N-C(7)	116.3 (3)	C(8)-C(7)-C(9)	109.7 (5)
-C(10)	115.5 (3)	N-C(10)-C(11)	109.0 (5)
C(7)-N-C(10)	125.2 (3)	N-C(10)-C(12)	108.3 (4)
O(1)-C(1)-O(2)	130.0 (3)	N-C(10)-C(13)	108.7 (4)
-C(2)	114.4 (3)	C(11)-C(10)-C(12)	108.7 (5)
O(2)-C(1)-C(2)	115.5 (3)	-C(13)	111.6 (4)
F(1)-C(2)-F(2)	108.4 (5)	C(12)-C(10)-C(13)	110.5 (5)
-F(3)	106.1 (5)	C(5)-C(13)-C(10)	113.2 (4)

[a] Hydrogen-bonded contacts are given by dotted bonds (···) between atoms in this and succeeding tables.

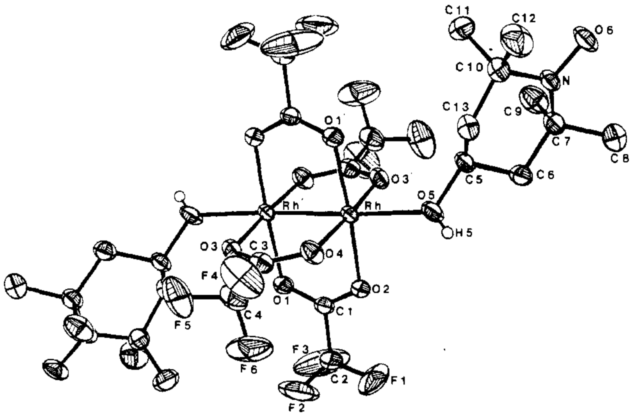

Figure 1. ORTEP drawing of $Rh_2(O_2CCF_3)_4(Tempol)_2$ (**1**) with thermal ellipsoids at the 30% probability level. The hydroxyl hydrogen atom H(5) is shown with an arbitrarily small thermal ellipsoid. The entire molecule resides on a crystallographic center of inversion at the midpoint of the Rh–Rh bond.

Table V. Bond Distances (Å) and Angles (Deg) for $Rh_2(O_2CCF_3)_4(H_2O)_2\cdot 2DTBN$ (**2**) Excluding the Hydrogen Atoms

Rh-Rh'	2.409 (1)	O(4)-C(3)	1.245 (4)
Rh-O(1)	2.034 (2)	O(5)···O(6)	2.799 (3)
Rh-O(2')	2.037 (2)	O(5)···O(6'')	2.776 (3)
Rh-O(3)	2.032 (2)	O(6)-N	1.261 (3)
Rh-O(4')	2.042 (2)	N-C(10)	1.494 (5)
-O(5)	2.243 (2)	N-C(20)	1.488 (5)
F(1)-C(2)	1.311 (4)	C(1)-C(2)	1.531 (4)
F(2)-C(2)	1.318 (4)	C(3)-C(4)	1.527 (4)
F(3)-C(2)	1.303 (4)	C(10)-C(11)	1.499 (13)
F(4)-C(4)	1.271 (5)	C(10)-C(12)	1.519 (7)
F(5)-C(4)	1.229 (5)	C(10)-C(13)	1.537 (9)
F(6)-C(4)	1.260 (5)	C(20)-C(21)	1.515 (7)
O(1)-C(1)	1.255 (4)	C(20)-C(22)	1.498 (9)
O(2)-C(1)	1.239 (4)	C(20)-C(23)	1.492 (10)
O(3)-C(3)	1.247 (4)		

Rh'-Rh-O(1)	87.93 (6)	O(1)-C(1)-C(2)	115.3 (3)
-O(2')	87.79 (6)	O(2)-C(1)-C(2)	114.9 (3)
-O(3)	87.97 (6)	F(1)-C(2)-F(2)	106.1 (3)
Rh'-Rh-O(4')	87.70 (6)	F(1)-C(2)-F(3)	108.6 (3)
Rh'-Rh-O(5)	178.75 (7)	F(1)-C(2)-C(1)	112.8 (3)
O(1)-Rh-O(2')	175.68 (7)	F(2)-C(2)-F(3)	107.7 (3)
O(1)-Rh-O(3)	87.21 (8)	-C(1)	112.4 (3)
-O(4')	92.19 (8)	F(3)-C(2)-C(1)	109.0 (3)
-O(5)	90.83 (9)	O(3)-C(3)-O(4)	129.7 (3)
O(2')-Rh-O(3)	93.27 (8)	O(3)-C(3)-C(4)	115.0 (3)
-O(4')	87.00 (8)	O(4)-C(3)-C(4)	115.2 (3)
-O(5)	93.45 (9)	F(4)-C(4)-F(5)	107.0 (4)
O(3)-Rh-O(4')	175.65 (7)	F(4)-C(4)-F(6)	103.7 (4)
O(3)-Rh-O(5)	91.86 (9)	-C(3)	112.6 (3)
O(4')-Rh-O(5)	92.46 (9)	F(5)-C(4)-F(6)	106.4 (4)
Rh-O(1)-C(1)	117.0 (2)	F(5)-C(4)-C(3)	115.7 (3)
Rh'-O(2)-C(1)	117.3 (2)	F(6)-C(4)-C(3)	110.6 (3)
Rh-O(3)-C(3)	117.3 (2)	N-C(10)-C(11)	106.2 (5)
Rh'-O(4)-C(3)	117.1 (2)	-C(12)	113.5 (4)
Rh-O(5)···O(6)	123.5 (1)	-C(13)	105.6 (5)
···O(6'')	127.3 (1)	C(11)-C(10)-C(12)	113.4 (9)
O(6)···O(5)···O(6'')	90.27 (9)	-C(13)	115.8 (1.1)
O(5)···O(6)···O(5'')	89.73 (9)	C(12)-C(10)-C(13)	102.2 (5)
O(5)···O(6)-N	137.0 (2)	N-C(20)-C(21)	112.3 (4)
O(5)···O(6'')-N''	132.9 (2)	N-C(20)-C(22)	109.4 (4)
O(6)-N-C(10)	114.7 (3)	N-C(20)-C(23)	108.0 (5)
-C(20)	115.7 (3)	C(21)-C(20)-C(22)	111.8 (6)
C(10)-N-C(20)	129.6 (3)	-C(23)	105.1 (6)
O(1)-C(1)-O(2)	129.7 (3)	C(22)-C(20)-C(23)	110.1 (8)

fluoroacetate), 116.9 (2)°; ∠F-C-F, 106.6 (5)°; ∠F-C-C, 112.2 (4)°; ∠O-C-O, 130.0 (3)°; ∠O-C-C, 115.0 (4)°. All of these dimensions, except those involving the fluorine atoms, are within six standard deviations of one another. The variations in the C–F distances (1.231–1.340 Å) and F–C–F (102.3–111.2°) and F–C–C (110.5–115.4°) angles arise from the highly anisotropic motion of the fluorine atoms and are suggestive of some minor amount of rotational disorder in the CF_3 groups,[6,8] although no actual evidence for this disorder was detected.

The Tempol ligands coordinate to the Rh atoms in **1** through their hydroxyl oxygen atoms at a distance of 2.240 (3) Å. As can be seen in Figure 2A, the piperidine ring of the Tempol ligand adopts a chair conformation, and consequently, the six ring atoms form a very distorted plane (Table VI[32]) with deviations as much as 0.75 Å. The N–O and C–O bonds of the Tempol ligand nearly bisect the molecule into two mirror images. The nitroxyl oxygen atom O(6) is displaced 0.409 Å out of the C(7)–N–C(10) plane (Table VI[32]). A useful gauge of planarity of the nitroxyl group C_2NO is given by the parameter α, where α is defined[33] as the angle between the N–O bond and the C–N–C plane. In **1** the nonplanar nitroxyl group is reflected by the α value of 18.6°.

Hydrogen-bonding interactions play a significant role in a description of the molecular packing for **1**, and the location and refinement of all hydrogen atoms in this compound afford

---

(33) Lajzerowicz-Bonneteau, J. In "Spin Labeling: Theory and Applications"; Berliner, L. J., Ed.; Academic Press: New York, 1976; pp 239–49.

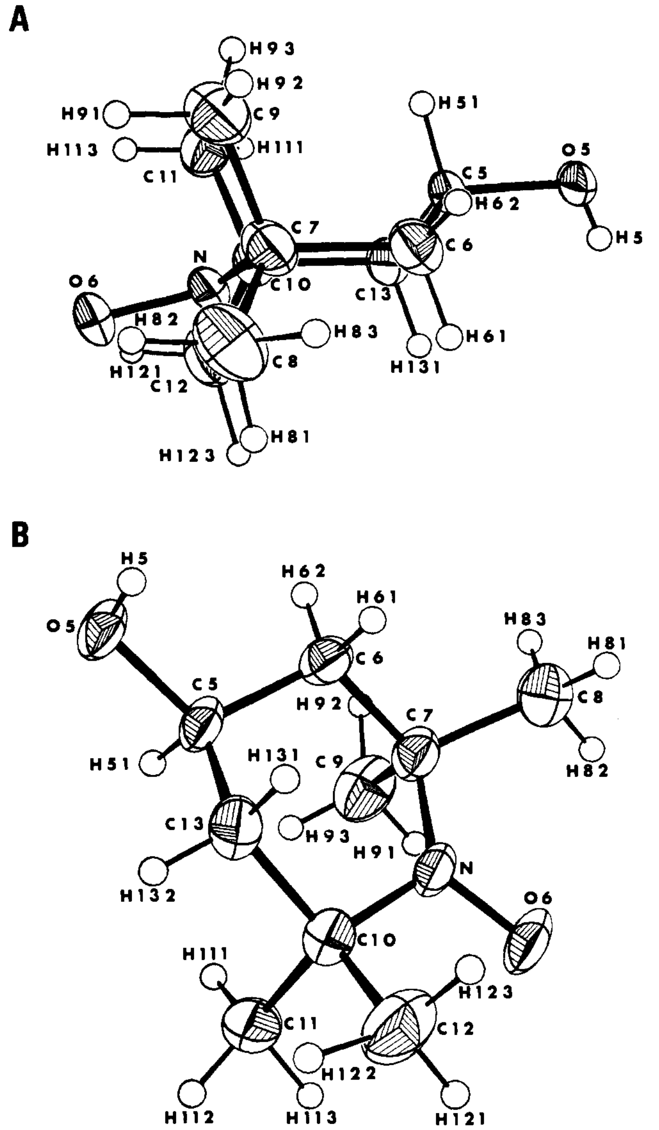

Figure 2. Two views of the Tempol axial ligand as found in **1** with vibrational ellipsoids drawn at the 30% probability level except for the hydrogen atoms, which are drawn with *B* values of 1.0 Å^2. View A shows the chair form of the piperidine ring with hydrogen atoms H(112), H(122), and H(132) obscured from view. View B gives a planar projection of the Tempol molecule with all atoms labeled.

an accurate picture of these interactions. The oxygen–oxygen contact, O(5)···O(6″), with a separation of 2.702 (4) Å between the axially coordinated hydroxyl oxygen atom and the nitroxyl oxygen atom from another Tempol ligand that is half of a unit cell away is indicative of the presence of a typical (2.6–2.8 Å) hydrogen bond. The hydroxyl hydrogen atom, H(5), as determined from the X-ray diffraction data presented here, is found to be located 0.69 (4) Å from O(5) and 2.01 (4) Å from the nitroxyl oxygen atom, O(6″). The hydrogen bond is very nearly linear with an O(5)–H(5)···O(6″) angle of 176 (5)° (Table VI[32]). The sp^2 hybridization at the nitroxyl oxygen atom O(6) is illustrated by the N–O(6)···H(5″) angle of 120 (1)°. Although only H(5) participates in the formation of hydrogen bonds in **1**, this interaction leads to a hydrogen-bonding network as shown in Figure 3. The dinuclear molecules are linked in a zigzag fashion in **1** into chains that extend approximately in the direction of the Rh–Rh vectors of each molecule. Since the $P2_1/n$ space group symmetry leads to two different directions for the Rh–Rh vectors, the hydrogen-bonded chains extend in two different directions throughout the lattice.

$Rh_2(O_2CCF_3)_4(H_2O)_2\cdot 2DTBN$ (2). One formula unit comprises the unit cell contents of **2** with the entire molecule located on a crystallographic center of inversion at the center of the Rh–Rh bond. The atom-labeling scheme is given in Figure 4. Four trifluoroacetate groups span the Rh–Rh bond of length 2.409 (1) Å in the usual fashion. The Rh atom is displaced by 0.076 Å out of the carboxylate oxygen plane (Table VI[32]), which includes O(1), O(2′), O(3), and O(4′). Representative bond distances and angles (mean values) within the $Rh_2(O_2CCF_3)_4$ unit include the following: Rh–O, 2.036 (2) Å; C–O, 1.247 (4) Å; C–CF_3, 1.529 (4) Å; C–F, 1.282 (5) Å; ∠Rh′–Rh–O(trifluoroacetate), 87.85 (6)°; ∠Rh–O–C, 117.2 (2)°; ∠F–C–F, 106.6 (4)°; ∠F–C–C, 112.2 (3)°; ∠O–C–O, 129.7 (3)°; ∠O–C–C, 115.1 (3)°. As was found in **1**, the anisotropic motion of the fluorine atoms leads to a range of bond distances and angles not observed among equivalent dimensions in the remainder of the molecule. Significant variations occur in the C–F distances (1.229–1.318 Å) and F–C–F (103.7–108.6°) and F–C–C (109.0–115.7°) angles due to the thermal motion of the fluorine atoms. As in the case of **1**, no evidence for disorder within the CF_3 groups was found.

The axial sites of the Rh atoms in **2** are occupied by oxygen atoms of the water molecules at a distance of 2.243 (2) Å. The $Rh_2(O_2CCF_3)_4(H_2O)_2$ molecule in **2** is depicted in Figure 5.[32] The Rh′–Rh–O(5) angle deviates only slightly from linearity with a value of 178.75 (7)°. The plane defined by the atoms of the water molecule [O(5), H(51), H(52)] forms a dihedral angle of 48.1° (Table VI[32]) with the equatorial carboxylate oxygen atom plane.

Two DTBN molecules, one of which is related by inversion symmetry to the other, are associated with each dirhodium(II) moiety in the crystal lattice. Each DTBN molecule has a pseudo-2-fold axis coincident with the N–O bond. In contrast to **1**, the nitroxyl oxygen atom lies nearly within the C(10)–N–C(20) plane showing a deviation of only 0.015 Å (Table VI[32]) from it. The nearly planar C_2NO fragment of the DTBN molecule is also reflected in the 0.7° angle for α. The methyl carbon atoms of the *tert*-butyl groups exhibit a

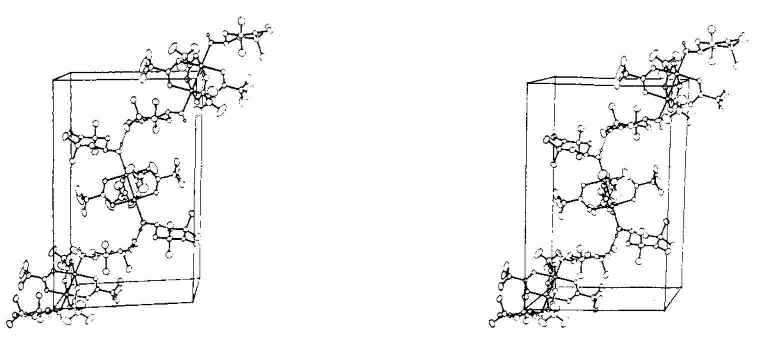

Figure 3. Stereoview of the unit cell contents in **1** showing the hydrogen-bonding network formed between the hydroxyl hydrogen atom H(5) and the nitroxyl oxygen atom O(6). Thermal ellipsoids enclosed 20% of their electron density except H(5), which is represented by a sphere of arbitrary size. The view is down the *a* axis with the *b* axis vertical, *c* axis horizontal, and the origin in the front upper right corner.

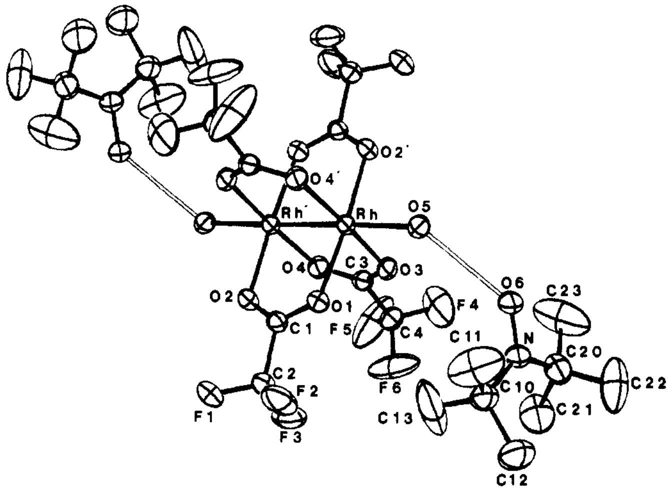

Figure 4. ORTEP drawing of $Rh_2(O_2CCF_3)_4(H_2O)_2{\cdot}2DTBN$ (**2**) with vibrational ellipsoids shown at the 30% probability level. The unfilled bonds represent the hydrogen-bonding interactions between the coordinated axial water molecules and the nitroxyl oxygen atoms O(6).

high degree of thermal motion, although no disorder was observed, and this is shown in the range of C–C distances (1.492–1.537 Å), C–C–N angles (105.6–113.5°), and esd's associated with these dimensions.

The principal intermolecular interactions in **2** are comprised of hydrogen bonding between the water and DTBN molecules. The oxygen–oxygen contact distances, O(5)···O(6) and O(5)···O(6″), are suggestive of hydrogen bonding with values of 2.799 (3) and 2.776 (3) Å, respectively. The refined hydrogen atom positions support this observation with O(5)–H(51) and O(5)–H(52) distances of 0.77 (4) and 0.74 (4) Å and hydrogen-bonding distances of H(51) and H(52) to a nitroxyl oxygen atom of 2.03 (4) and 2.06 (4) Å, respectively. As can be seen from the hydrogen bond depicted in Figure 4, only one hydrogen atom [H(52)] is primarily associated with each DTBN oxygen atom although H(51) is only 2.92 (4) Å away. Thus, H(51) is more closely bonded to a DTBN oxygen atom [O(6″)] on an adjacent molecule in the lattice. The hydrogen-bonding angles also reflect this tendency of each hydrogen atom of the water molecules to interact with only one nitroxyl oxygen atom. The O(5)–H(51)···O(6″) and O(5)–H(52)···O(6) angles of 161 (4) and 176 (5)°, respectively, represent genuine hydrogen-bonding contacts approaching linearity while the O(5)–H(51)···O(6) and O(5)–H(52)···O(6″) angles of 73 (3) and 74 (3)°, respectively, do not correspond to normal hydrogen-bond angles. The net result of the hydrogen-bonding interactions between water and DTBN molecules affords a zigzagging hydrogen-bonding network connecting adjacent $Rh_2(O_2CCF_3)_4(H_2O)_2$ molecules through the oxygen atoms of the DTBN nitroxyl groups.

In both compound **1** and compound **2** the hydrogen-bonding interactions represent the only significant intermolecular contacts. Fluorine–fluorine contacts, which were found to be close to twice the van der Waals radius of fluorine (1.40 Å[34]) in $Rh_2(O_2CCF_3)_4(EtOH)_2$[14] and $Rh_2(O_2CCF_3)_4(Me_2SO_2)_2$,[24] are not found at less than 3 Å in **1** and **2**. However, it should be noted that, in structures involving the trifluoromethyl group, some amount of artificial shortening of the fluorine–fluorine contacts undoubtedly occurs from the large thermal parameters associated with these fluorine atoms.

Discussion

Although previous studies[35–38] have examined some of the factors governing adduct formation in tetrakis(carboxylato)dirhodium(II) complexes, none of these studies have involved the trifluoroacetate bridging group, which, as noted in the Introduction, can control the identity of the axial donor atom coordinating to the rhodium atom. With an ambidentate ligand like Me_2SO,[21,22] the highly electron-withdrawing CF_3 substituents lead to the rhodium atom favoring the less polarizable oxygen atom for axial ligation over the sulfur atom, whereas electron-donating substituents like CH_3 or C_2H_5 lead to sulfur atom coordination. In compounds **1** and **2** the axial ligands for $Rh_2(O_2CCF_3)_4$ are oxygen donors but not from the nitroxyl groups as originally intended. In **1** the 4-hydroxyl substituent of the Tempol ligand successfully competes for axial coordination with the nitroxyl moiety, resulting in a 2:1 adduct with $Rh_2(O_2CCF_3)_4$ rather than a 1:1 adduct in which both hydroxyl and nitroxyl groups participate in direct coordination. The latter type of complex has been found in $Cu(hfac)_2(Tempol)$[28] when stoichiometric quantities of $Cu(hfac)_2$ and Tempol are combined in a noncoordinating solvent. Compound **2** was first isolated as dark green crystals (see Experimental Section), which presumably contain coordinated DTBN molecules in the axial positions of $Rh_2(O_2CCF_3)_4$. After recrystallization in excess DTBN, these crystals produce dichroic blue-red crystals (**2**) over a 1-week period in air, which contain water molecules at the axial sites of $Rh_2(O_2CCF_3)_4$. However, the DTBN molecules remain "trapped" in the crystal lattice. The structures of both **1** and **2** suggest that the nitroxyl oxygen atoms function as relatively weak donors compared to the 4-hydroxy substituent of Tempol or H_2O. The bonding interactions in **1** and **2** are explicable in terms of largely independent nitroxyl groups with their associated hydrogen bonding and $Rh_2(O_2CCF_3)_4$ molecules with the axial ligands connecting these dinuclear units to the hydrogen-bonding networks throughout the crystal lattices. A more detailed discussion of the bonding in the nitroxyl groups and the $Rh_2(O_2CCF_3)_4$ units will now be given with an emphasis on comparisons with known structures.

Table VII. Comparison of Nitroxyl Group Geometries in Tempol and DTBN

compd	N–O, Å	C–N–C, deg	α,[a] deg	ref
Tempol	1.291 (7)	125.4 (5)	15.8	39
$Cu(hfac)_2(Tempol)$	1.276 (8)	126.7 (6)	5.2	28
$Rh_2(O_2CCF_3)_4(Tempol)_2$	1.282 (4)	125.2 (3)	18.6	this work
DTBN[b]	1.280 (20)	136 (3)	0.0[c]	42
$Rh_2(O_2CCF_3)_4(H_2O)_2{\cdot}$ 2DTBN	1.261 (3)	129.6 (3)	0.7	this work

[a] Out-of-plane acute angle between the N–O bond and the C–N–C plane. This angle defines the conformation of the C_2NO group. [b] Structure determined by gas-phase electron diffraction. [c] This angle could not be experimentally determined but was taken as 0°.

Nitroxyl Group Geometries and Hydrogen Bonding. Table VII presents a collection of bond distances and angles that define the geometry of the nitroxyl groups in Tempol and DTBN. The N–O bond length in **1** of 1.282 (4) Å is within the range of values found for the Tempol molecule itself[39] [1.291 (7) Å] and $Cu(hfac)_2(Tempol)$[28] [1.276 (8) Å]. The nitroxyl groups in Tempol and in **1** participate in hydrogen-bonding interactions (vide infra), while in $Cu(hfac)_2(Tempol)$ the nitroxyl moiety is directly coordinated to the copper atom

---

(34) Zefirov, Yu. V.; Porai-Koshits, M. A. *Zh. Strukt. Khim.* **1980**, *21*, 150; *J. Struct. Chem. (Engl. Transl.)* **1980**, *21*, 526.
(35) Das, K.; Simmons, E. L.; Bear, J. L. *Inorg. Chem.* **1977**, *16*, 1268.
(36) Bear, J. L.; Howard, R. A.; Korn, J. E. *Inorg. Chim. Acta* **1979**, *32*, 123.
(37) Drago, R. S.; Tanner, S. P.; Richman, R. M.; Long, J. R. *J. Am. Chem. Soc.* **1979**, *101*, 2897.
(38) Drago, R. S.; Long, J. R.; Cosmano, R. *Inorg. Chem.* **1981**, *20*, 2920.
(39) Berliner, L. J. *Acta Crystallogr., Sect. B* **1970**, *B26*, 1198.

Table VIII. Selected Structural Parameters in $Rh_2(O_2CCF_3)_4L_2$ Complexes[a]

L	Rh-Rh, Å	Rh-L, Å	Rh-O, Å	Δ,[b] Å	C-O, Å	Rh-Rh-O, deg	Rh-O-C, deg	O-C-O, deg	ref
Me_2SO_2	2.400 (1)	2.287 (3)	2.031 (3)	0.071	1.251 (6)	88.00 (9)	117.5 (3)	128.9 (5)	24
EtOH	2.402 (2)	2.27 (1)	2.03 (1)	0.073	1.25 (2)	87.9 (3)	118 (1)	129 (2)	14
Tempol	2.405 (1)	2.240 (3)	2.034 (2)	0.070	1.250 (4)	88.02 (7)	116.9 (2)	130.0 (3)	this work
$Me_2SO\text{-}d_6$	2.408 (1)	2.248 (3)	2.035 (3)	0.076	1.249 (5)	87.87 (8)	117.5 (2)	129.3 (4)	22
H_2O[c]	2.409 (1)	2.243 (2)	2.036 (2)	0.076	1.246 (4)	87.85 (6)	117.2 (2)	129.7 (3)	this work
Me_2SO	2.420 (1)	2.240 (3)	2.031 (3)	0.085	1.249 (5)	87.65 (8)	117.9 (2)	128.8 (4)	21, 22
$P(OPh)_3$	2.470 (1)	2.422 (2)	2.041 (5)	0.110	1.247 (9)	86.9 (2)	118.7 (5)	128.9 (8)	47
PPh_3	2.486 (1)	2.494 (2)	2.045 (5)	0.125	1.245 (8)	86.9 (1)	119.3 (5)	128.2 (7)	47

[a] Equivalent distances and angles have been averaged when appropriate. [b] Out-of-plane displacement of the Rh atom from the equatorial carboxylate oxygen atom plane. [c] As found in $Rh_2(O_2CCF_3)_4(H_2O)_2 \cdot 2DTBN$.

at one of the axial positions in this tetragonally elongated chain structure. The N–O bond length (1.283 ± 0.008 Å) in $Cu(hfac)_2(Tempol)$ appears to be unaffected by bond formation between the nitroxyl oxygen and copper atoms. The range of C–N–C angles (125.2–126.7°) in the three Tempol molecules in Table VII is in accord with the values found in structures of similar organic nitroxides[33,40] in which the nitroxyl group is unconstrained in a six-membered ring. On the other hand, significant variations in the C–N–C angle can be effected by means of a change in the size of the aliphatic ring. The highly strained bicyclic compound 1,5-dimethyl-8-azabicyclo[3.2.1]octan-3-one-8-oxyl[41] reduces the C–N–C angle to only 107.4 (3)°. The angle α represents a gauge of the deviation from planarity of the nitroxyl oxygen atom from the C_2N group. In Tempol and $Rh_2(O_2CCF_3)_4(Tempol)_2$ the value of α ranges between 15 and 20°, which is typical for a chair conformation of the Tempol ring. The α value of 5.2° in $Cu(hfac)_2(Tempol)$ reflects a flattening of the ring, which, in conjunction with the observed thermal parameters associated with the central portion of the Tempol ring, is suggestive of a static or dynamic disorder that arises from two slightly different conformations of the Tempol ring.[28]

Previous structural data on DTBN have been limited to that obtainable at 70 °C in the gas phase by electron diffraction,[42] and the dimensions reported in Table VII were determined in that study. The structure of DTBN in **2** constitutes, to the best of our knowledge, the first example in which this molecule has been characterized in the solid state with X-ray diffraction. As can be seen from the N–O bond lengths, C–N–C angles, and α values shown in Table VII, the gas-phase structure of DTBN at 70 °C and the solid-state structure of DTBN in **2** at 26 °C are essentially identical within the statistical uncertainties of the data. In contrast to the C–N–C angles involving the Tempol molecules in Table VII, the C–N–C angle in **2** opens up to 129.6 (3)°. Acyclic nitroxides, however, do not always show an increase in the C–N–C angle over that found in cyclic nitroxides, and as an example, perchlorodiphenyl nitroxide[43] shows a C–N–C angle of only 119.9 (1)°. The chair conformation of the cycloaliphatic ring in Tempol results in significantly nonzero α values for the C_2NO group, whereas this same group assumes a nearly planar geometry in DTBN with the α value very close to 0° in **2**. In the structure of DTBN determined in the vapor phase,[42] the molecule was assumed to have a 2-fold symmetry axis coincident with the N–O bond that fixes α as exactly 0°. Electronic structure calculations on the aminoxyl (H_2NO) group[44] do not suggest a well-defined overall geometry, and consequently, the orientation of the N–O bond relative to the C_2N plane is controlled principally by the carbon atom substituents.

Although the nitroxyl groups in **1** and **2** do not coordinate directly to the rhodium atoms, each nitroxyl oxygen atom participates in hydrogen bonding to the most acidic proton in each structure. A recent analysis[45] of the intermolecular contacts in the structures of 15 aliphatic nitroxides led to the conclusion that "when there is a possibility of intermolecular hydrogen bonding, it always exists". If the nitroxyl oxygen atom is denied access to a proton through which it can form a hydrogen bond [O(nitroxide)···X < 3 Å for X = O, N, C], then short contacts (3.0–3.4 Å) typically will exist between the nitroxyl oxygen atom and the carbon atoms of methyl or methylene groups.[45] In both **1** and **2** hydrogen bonds of the type O–H···O(nitroxide) are found with O···O(nitroxide) separations between 2.7 and 2.8 Å.

In a theoretical evaluation of the electrostatic potential about the aminoxyl molecule, Ellinger et al.[46] found that the approach of a proton is most favorable when it occurs in the direction of the oxygen atom lone pairs of the nitroxyl group. To a certain extent, this preferred bonding of the nitroxyl group can be seen in the structures of $Cu(hfac)_2(Tempol)$[28] and $Cu(hfac)_2(Tempo)$,[29] which both have a nitroxyl group coordinated to the Lewis acid $Cu(hfac)_2$. The Tempol complex has a Cu–O–N angle of 170.1 (5)° and a Cu–O(nitroxide) distance of 2.439 (6) Å, while the Tempo complex has a Cu–O–N angle much closer to that expected for an sp^2-hybridized oxygen atom with a value of 123.9 (4)° and a corresponding Cu–O(nitroxide) distance of 1.920 (5) Å. However, the significance of this comparison is blurred by the change in coordination number for the two complexes, which undoubtably accounts for some of the shortening in the Cu–O(nitroxide) distance in the Tempo complex. In both **1** and **2** the essentially sp^2 hybridization about the nitroxyl oxygen atoms is manifested in the N–O···H angles in **1** [120 (1)°] and **2** [132 (1) and 137 (1)°], and the values of these angles strongly suggest that mainly σ bonding occurs between the nitroxyl oxygen and hydrogen atoms.

Bonding in $Rh_2(O_2CCF_3)_4L_2$ Complexes. With the structures of **1** and **2** reported here, altogether eight diadducts of $Rh_2(O_2CCF_3)_4$ have been characterized in detail by X-ray crystallography including L = Me_2SO_2,[24] EtOH,[14] Tempol, $Me_2SO\text{-}d_6$,[22] H_2O, Me_2SO,[21,22] $P(OPh)_3$,[47] and PPh_3.[47] Pertinent structural data are assembled in Table VIII. The range of Rh-Rh distances (0.086 Å) in $Rh_2(O_2CCF_3)_4L_2$ complexes represents about 10% of the total range (0.796 Å) encompassed by all $M_2(O_2CCF_3)_4L_2$ complexes with syn–syn trifluoroacetate bridging groups. Among $Rh_2(O_2CR)_4L_2$ complexes, those with R = CF_3 have Rh–Rh distances over about 75% of the total range bounded by $Rh_2(O_2CCMe_3)_4(H_2O)_2$[20] at 2.371 (1) Å and $Rh_2(O_2CCF_3)_4(PPh_3)_2$[47] at 2.486 (1) Å. It is to be noted

---

(40) Shibaeva, R. N. *Zh. Strukt. Khim.* **1975**, *16*, 330; *J. Struct. Chem.* (*Engl. Transl.*) **1975**, *16*, 318.

(41) Capiomont, A. *Acta Crystallogr., Sect. B* **1973**, *B29*, 1720.

(42) Andersen, B.; Andersen, P. *Acta Chem. Scand.* **1966**, *20*, 2728.

(43) Solans, X.; Goli, S.; Miravitlles, C.; Font-Altaba, M. *Acta Crystallogr., Sect. B* **1978**, *B34*, 2331.

(44) Salotto, A. W.; Burnelle, L. *J. Chem. Phys.* **1970**, *53*, 333.

(45) Chion, B.; Lajzerowicz-Bonneteau, J. *Acta Crystallogr., Sect. B* **1980**, *B36*, 998.

(46) Ellinger, Y.; Subra, R.; Berthier, G.; Tomasi, J. *J. Phys. Chem.* **1975**, *79*, 2240.

(47) Cotton, F. A.; Felthouse, T. R.; Klein, S. *Inorg. Chem.* **1981**, *20*, 3037.

that the identity of the axial donor ligand is far more effective in changing the Rh–Rh bond length than is the carboxylate R-group substituent. In the series of five dinuclear complexes with the general formula $Rh_2(O_2CR)_4(H_2O)_2$, the Rh–Rh bond lengths of 2.371 (1) Å (R = CMe_3[20]), 2.378 (1) Å (R = O^-[48]), 2.3855 (5) Å (R = Me[5]), 2.386 (3) Å (R = $CH_2CH_2NH_3^+$[49]), and 2.409 (1) Å (R = CF_3) span only 0.038 Å, whereas the substitution of PPh_3 for H_2O in $Rh_2(O_2CMe)_4$[50] and $Rh_2(O_2CCF_3)_4$[47] leads to an increase in the Rh–Rh distances of 0.065 and 0.077 Å, respectively. An assessment of the factors controlling the Rh–Rh bond length, however, must include electronic effects transmitted by the axial ligands[51] as well as the carboxylate R-group substituents and steric interactions[47] between the axial ligands and the $Rh_2(O_2CR)_4$ unit.

Several years ago, prior to the appearance of any structural data on $Rh_2(O_2CCF_3)_4L_2$ complexes, Koh and Christoph[52] examined several structural parameters for dimetal tetracarboxylates, correlated these data with the metal–metal distances, and compared these correlations with the corresponding ones for various $Rh_2(O_2CMe)_4L_2$ complexes. The data contained in Table VIII display similar trends for the $Rh_2(O_2CCF_3)_4L_2$ complexes. The Rh–O(carboxylate) and C–O distances are practically invariant with values of 2.035 ± 0.005 and 1.248 ± 0.002 Å, respectively. As noted before,[52] the angles about the five-membered $\overline{\text{Rh–Rh–O–C–O}}$ ring respond most noticeably to changes in the Rh–Rh bond length. The Rh–Rh–O and Rh–O–C angles show decreases and increases, respectively, as the Rh–Rh distance lengthens, although these changes are scarcely above the level of statistical significance. The Rh–Rh–O angles gradually decrease from 88.00 (9)° for L = Me_2SO_2 in $Rh_2(O_2CCF_3)_4L_2$ complexes to 86.9 (1)° for L = PPh_3 with an average of 87.6 ± 0.5°. The trend becomes more apparent when other $Rh_2(O_2CR)_4L_2$ complexes are included and persists even over a wide range of $M_2(O_2CR)_4L_2$ compounds, yielding an excellent linear correlation[52] between the M–M–O angle and the M–M distance. The correlation between the Rh–O–C angles and the Rh–Rh distance is in the direction opposite to that of the Rh–Rh–O angles with an increase from 117.5 (3)° for L = Me_2SO_2 to 119.3 (5)° for L = PPh_3, although no systematic trend in the M–O–C angle is evident over a wide range of $M_2(O_2CR)_4L_2$ complexes.[52] The magnitude of the out-of-plane displacement (Δ) in Table VIII of the Rh atom from the equatorial carboxylate oxygen plane reflects a combination of the invariability of the C–O distance and a gradual decrease in the Rh–Rh–O angle as the Rh–Rh bond lengthens to produce an almost monotonic increase from 0.071 Å for L = Me_2SO_2 to 0.125 Å for L = PPh_3. The direction of this increase in Δ is toward the axial donor ligands since the lengths of the Rh–Rh bonds exceed the carboxylate O···O separations [e.g., 2.265 (4) and 2.256 (3) Å in **1** and **2**, respectively].

The most prominent deviations in the carboxylate-group geometry for $Rh_2(O_2CR)_4L_2$ compounds over other dimetal tetracarboxylates occur in the size of the O–C–O angle. The series of eight $Rh_2(O_2CCF_3)_4L_2$ complexes in Table VIII has an average O–C–O angle of 129.1 ± 0.6°, which exceeds the values found not only in other $M_2(O_2CR)_4L_2$ complexes but in other $Rh_2(O_2CR)_4L_2$ compounds as well.[52] Among dirhodium tetracarboxylates, the trifluoroacetate complexes presumably have larger O–C–O angles because the electron-withdrawing character of the CF_3 group decreases the electron density on the carboxyl carbon atom. Since *all* $Rh_2(O_2CR)_4L_2$ compounds consistently show larger O–C–O angles, the implication exists that the carboxylate ligands foster bonding interactions within the Rh_2^{4+} moiety that do not occur in the absence of these bridging ligands.[52] Evidence for enhanced π interactions between the carboxylate bridges and the Rh_2^{4+} unit comes from both theoretical calculations and experimental data. Norman and Kolari[53] discovered in their SCF–Xα–SW calculations on $Rh_2(O_2CH)_4(H_2O)_2$ that extensive mixing between the carboxylate oxygen and rhodium atomic orbitals occurs. Bear et al.[54] reported that the X-ray photoelectron spectrum of $Rh_2(O_2CCH_3)_4$ shows an increase in the C 1s binding energy for the acetyl over the methyl carbon atoms, which was attributed to an increase in the electron density at the acetyl carbon atoms. Both of the above reports provide possible explanations for the unusually large O–C–O angles that are characteristic in $Rh_2(O_2CR)_4L_2$ complexes.

The bond lengths within the L–Rh–Rh–L fragment in **1** and **2** agree closely with the four other $Rh_2(O_2CCF_3)_4L_2$ structures having axial oxygen-donor ligands shown in Table VIII. Average Rh–Rh and Rh–O distances within this set of six $Rh_2(O_2CCF_3)_4L_2$ complexes are 2.407 ± 0.007 and 2.255 ± 0.019 Å, respectively. These values are correspondingly longer and shorter than those in other $Rh_2(O_2CR)_4L_2$ complexes with axial oxygen ligands due to the enhanced Lewis acidity of the rhodium atoms by the CF_3 groups. In a molecular orbital sense, the effect of the CF_3 groups appears to be a lowering in energy of the primarily metal orbitals leading to a more favorable interaction (energetically closer) with the axial oxygen atom lone pairs. Electrochemical data[17] substantiate this orbital stabilization effect by the CF_3 substituents for *both* axial oxygen and phosphorus donor atoms although in the latter case the electronic ground state (HOMO) has changed from Rh–Rh δ^* to Rh–Rh σ.[51] Concomitant with this change in the HOMO is a lengthening of the Rh–Rh bond for L = PR_3 to ca. 2.48 Å.

Several years ago, a linear correlation was proposed between the Rh–Rh distance and the pK_b value of the axial ligand.[55] Although this relationship appears to have been fortuitous, it was recognized that phosphine ligands deviated strongly from the linear correlation between the Rh–Rh distance and pK_b value. Recent Xα–SW calculations[51] suggest that the origin of this strong deviation lies in the change of ground-state orbitals (an implicit assumption required for a correlation between Rh–Rh distance and pK_b is that these orbitals do *not* reorder) in going from oxygen to phosphorus axial ligands and is *not* due to any π-back-bonding effects with the donor atoms. It is this orbital rearrangement of the HOMO in $Rh_2(O_2CR)_4L_2$ complexes that accounts for the grouping of Rh–Rh distances in Table VIII about 2.41 ± 0.01 (L = O-donor atom) and 2.48 ± 0.01 Å (L = P-donor atom). Within these two groups, variations in the Rh–L distances occur because of a combination of electronic, steric, and molecular packing effects. The inductive effect of the CF_3 group perturbs the Rh–Rh ground state to a lesser degree than that of the axial ligand except for the unusual case with the ambidentate Me_2SO ligand in which oxygen and not sulfur coordinates to the rhodium atom.[21,22]

Acknowledgment. We thank the Robert A. Welch Foundation (Grant No. A-494) for financial support and Engelhard Industries for a loan of rhodium trichloride.

Registry No. **1**, 81371-96-2; **2**, 81371-97-3; $Rh_2(O_2CCF_3)_4$, 31126-95-1.

---

(48) Cotton, F. A.; Felthouse, T. R. *Inorg. Chem.* **1980**, *19*, 320.

(49) Korp, J. D.; Bernal, I.; Bear, J. L. *Inorg. Chim. Acta* **1981**, *51*, 1.

(50) Christoph, G. G.; Halpern, J.; Khare, G. P.; Koh, Y. B.; Romanowski, C. *Inorg. Chem.* **1981**, *20*, 3029.

(51) Bursten, B. E.; Cotton, F. A. *Inorg. Chem.* **1981**, *20*, 3042.

(52) Koh, Y. B.; Christoph, G. G. *Inorg. Chem.* **1979**, *18*, 1122.

(53) Norman, J. G., Jr.; Kolari, H. J. *J. Am. Chem. Soc.* **1978**, *100*, 791.

(54) Dennis, A. M.; Howard, R. A.; Kadish, K. M.; Bear, J. L.; Brace, J.; Winograd, N. *Inorg. Chim. Acta* **1980**, *44*, L139.

(55) Koh, Y. B.; Christoph, G. G. *Inorg. Chem.* **1978**, *17*, 2590.

Supplementary Material Available: Tables of anisotropic thermal parameters for **1** (Table IIA), anisotropic thermal parameters for **2** (Table IIIA), bond distances and angles involving the hydrogen atoms in **1** (Table IVA), bond distances and angles involving the hydrogen atoms in **2** (Table VA), least-squares planes and dihedral angles (Table VI), and observed and calculated structure factors for **1** and **2** and Figure 5 (ORTEP drawing of $Rh_2(O_2CCF_3)_4(H_2O)_2$) (37 pages). Ordering information is given on any current masthead page.

Contribution from the Department of Chemistry,
Texas A&M University, College Station, Texas 77843

New Trinuclear, Oxo-Centered, Basic Carboxylate Compounds of Transition Metals. 1. Trichromium(II,III,III) Compounds

F. ALBERT COTTON* and WENNING WANG

Received November 30, 1981

The preparation and structural characterization of two compounds of general formula $Cr_3(\mu_3\text{-}O)(O_2CCF_2H)_6L_3\cdot$(solvent) is reported, viz., compound **1** with L = pyridine and solvent = $(C_2H_5)_2O$ and compound **2** in which L = 4-cyanopyridine and solvent = toluene. These are the first compounds containing a planar-triangular Cr_3O moiety in a neutral rather than cationic $Cr_3O(O_2CR)_6L_3$ unit. Formally the chromium atoms are in oxidation states of II, III, and III, but the structures have 3-fold symmetry, which indicates that the three metal atoms are electronically equivalent as a result of electron delocalization. Some important intramolecular distances, given in each case in angstroms for compounds **1** and **2** in that order, are as follows: Cr···Cr, 3.356 (2), 3.336 (1); Cr–(μ_3-O), 1.938 (1), 1.926 (1); Cr–N, 2.158 (7), 2.155 (5); Cr–O(carboxyl), 2.034 [7], 2.028 [4]. The crystallographic parameters are as follows. Compound **1**: space group $R32$; a = 18.149 (4) Å; c = 10.675 (3) Å; Z = 3; refined to R_1 = 0.069 and R_2 = 0.081. Compound **2**: space group $R\bar{3}c$; a = 16.422 (2) Å; c = 60.227 (8) Å; Z = 12; refined to R_1 = 0.080 and R_2 = 0.097.

Introduction

In this and several papers to follow we shall present new results on trinuclear complexes of the structural type shown in Figure 1. The essential components of this structure are the equilateral triangle of metal atoms with an oxygen atom at the center, the six edge-bridging carboxyl groups, and the three equatorial ligands, L. The ideal structure has D_{3h} symmetry and may also be described approximately as three octahedra sharing a common vertex, which is the central oxygen atom. It is to be emphasized that species with this structure are not metal atom cluster compounds. With the μ_3-O atom lying in the plane of the M_3 triangle, the M–(μ_3-O) bonds, even though they are rather short, require the metal atoms to be so far from one another ($\gtrsim$3.3 Å) that for M^{II} and/or M^{III} atoms no significant M–M bonding is possible.

Although several compounds of this type have been known for more than half a century, it is only since about 1969 that structural information has become available through X-ray crystallography, first, in approximate form, for $[Fe_3O(O_2CCH_3)_6(H_2O)_3]ClO_4$[1] and $[Mn_3O(O_2CCH_3)_6(CH_3CO_2)_{2/2}(CH_3COOH)]$.[2] In 1970 the first accurate structure was reported for $[Cr_3O(O_2CCH_3)_6(H_2O)_3]Cl\cdot 6H_2O$.[3] In each of these compounds all three metal atoms are formally M^{III}, so that their structural equivalence is not unexpected. In 1972 the first example of a compound having L other than H_2O and metal atoms in formal oxidation states II, III, and III was reported,[4] namely, $Ru_3O(O_2CCH_3)_6(PPh_3)_3$. Here there was the possibility that the different oxidation states might be trapped, but the structure appears to have genuine 3-fold symmetry. Since then three more II, III, III structures have been reported, namely, for $M_3O(O_2CCH_3)_6(py)_3$ with M = Mn[5] and Fe[6] and for $Mn_3O(O_2CCH_3)_6[3\text{-}Cl(py)]_3$.[7] In the first two, there appears to be full 3-fold symmetry, but in the last one there is, undoubtedly, a trapping of the valences.

Of all these compounds, the chromium compound has been most thoroughly studied both magnetically[8] and spectroscopically,[9] although the two manganese compounds have been subjected to detailed magnetic study.[10] All of the data for the chromium compound were satisfactorily explained by a model in which there is weak coupling between localized d^3 configurations, presumably through the central μ_3-O atom.

We have recently isolated two compounds of the type under consideration in which there are chromium atoms with formal oxidation numbers II, III, and III. We have investigated their structures to determine the effect of having mixed oxidation states (or, from another point of view, introducing one more electron into the III, III, III system), particularly to see if any valence trapping might occur. These two new compounds contain O_2CCF_2H groups and have either pyridine (**1**) or 4-cyanopyridine (**2**) as equatorial ligands.

Experimental Section

Reactions and manipulations involving oxidation-sensitive chromium(II) solutions and compounds were carried out under atmospheres of nitrogen or, in the case of selecting and mounting crystals for X-ray studies, under a layer of heavy, degassed mineral oil. The compounds studied are also moisture sensitive, and appropriate precautions were taken to exclude water from the reaction systems.

To a suspension of 1.3 g (2.8 mmol) of $(NH_4)_4[Cr_2(CO_3)_4(H_2O)_2]$[11] in 50 mL of diethyl ether was added 1.0 mL (16 mmol) of CF_2HCOOH. The mixture was refluxed for 2 h to convert the slurry of the yellow carbonate complex to a purple solution. The solvent was then stripped from the solution, and the residue was dried for 16 h under

---

(1) Anzenhofer, K.; de Boer, J. J. *Recl. Trav. Chim. Pays-Bas* **1969**, *88*, 286.

(2) Hessel, L. W.; Romers, C. *Recl. Trav. Chim. Pays-Bas* **1969**, *88*, 545.

(3) Chang, S. C.; Jeffrey, G. A. *Acta Crystallogr., Sect. B* **1970**, *B26*, 673.

(4) Cotton, F. A.; Norman, J. G., Jr. *Inorg. Chim. Acta* **1972**, *6*, 411.

(5) Baikie, A. R. E.; Hursthouse, M. B.; New, D. B.; Thornton, P. *J. Chem. Soc., Chem. Commun.* **1978**, 62.

(6) See Table III in: Catterick, J.; Thornton, P. *Adv. Inorg. Chem. Radiochem.* **1977**, *20*, 291.

(7) Baikie, A. R. E.; Hursthouse, M. B.; New, L.; Thornton, P.; White, R. G. *J. Chem. Soc., Chem. Commun.* **1980**, 684.

(8) Earnshaw, A.; Figgis, B. N.; Lewis, J. *J. Chem. Soc. A* **1966**, 1656.

(9) (a) Dubicki, L.; Martin, R. L. *Aust. J. Chem.* **1969**, *22*, 701. (b) Dubicki, L.; Day, P. *Inorg. Chem.* **1972**, *11*, 1868.

(10) Thornton, P., private communication.

(11) Cotton, F. A.; Rice, G. W. *Inorg. Chem.* **1978**, *17*, 2004.